

# High-Temperature Fibre Optical Sensor

R.D. Pechstedt, A. Sposito

*Oxsensis Ltd., Unit 6, Genesis Building, Library Avenue, Harwell Campus, Didcot, Oxfordshire, OX11 0SG*  
*ralf.pechstedt@oxsensis.com*

**Abstract:** we report a sapphire Fabry-Perot cavity based fibre optical temperature sensor that is capable of operating at elevated temperatures  $> 1000^{\circ}\text{C}$  for prolonged periods of time. The sensing cavity is mounted at the front end of an extended alumina tube and is illuminated by a collimated light beam, thus separating the hot zone from the optical fibre lead. Stability to  $\pm 1^{\circ}\text{C}$  at  $1100^{\circ}\text{C}$  over 42 days has been demonstrated, together with a resolution  $< 0.5^{\circ}\text{C}$  at  $1300^{\circ}\text{C}$ .

**OCIS codes:** (060.2370) Fiber optics sensor; (120.2230) Fabry-Perot; (120.3180) Interferometry; (120.6780) Temperature

## 1. Introduction

There is great interest in accurate measurements of high to ultra-high temperatures around and above  $1000^{\circ}\text{C}$ . Industrial applications include monitoring and optimizing of combustion processes in gas turbines to enhance fuel efficiency and flexibility whilst simultaneously reducing emission, increasing energy efficiency of high-temperature steel production processes, ensuring quality control of molten glass processing during production and in-pile temperature monitoring in next generation nuclear reactors. These are very harsh conditions due to extreme temperatures, corrosive environments and high radiation levels. Conventional thermocouples (TC) are therefore only of limited use in these applications, often limited in lifetime, loss of accuracy or requiring excessive protection. For example, Nickel based mineral insulated metal sheathed thermocouples start to exhibit significant drift when operated above  $1000^{\circ}\text{C}$  [1]. Silica fibre optical sensor can be used to overcome some of the above challenges; however these are usually restricted to temperatures below  $1000^{\circ}\text{C}$ . For example, drift observed in a silica fibre based Fabry-Perot sensor has been tracked down to germanium out diffusion from the core into the cladding, creating second order mode interference effects [2]. Growth of crystalline structures within or on the surface of amorphous glass fibre can lead to structural changes at temperature above  $1200^{\circ}\text{C}$  during prolonged exposure [3]. Sapphire with its high melting point of  $2050^{\circ}\text{C}$  seems to be the ideal candidate for extending the upper temperature limit. Indeed, Fibre Bragg Gratings written into sapphire fibre have been used to demonstrate record working temperatures of up to  $1900^{\circ}\text{C}$  [4]. However, writing first order gratings with a reflection peak in the  $1550\text{nm}$  window requires specialist equipment and set-up [5] and is not yet widely available. Further, supply of sapphire fibre is limited to a small number of vendors which may be a concern for commercial applications.

Here we report a high-temperature sensor prototype based on a sapphire Fabry-Perot (FP) cavity that employs materials readily available and that is capable to operate at temperatures above  $1000^{\circ}\text{C}$  for extended periods of time.

## 2. Operating principle

The sensor is based on a FP cavity formed by a thin sapphire plate with parallel surfaces that is attached to a long alumina tube [6]. This forms the hot end of the sensor, whereas the opposite end is kept at considerably lower temperature during operation. A lens is employed to collimate light emanating from the single-mode lead fibre and delivers a near planar wavefront to the FP. The FP interference is created by the Fresnel reflections of about 7% at the sapphire to air interfaces without the need to deposit any reflective layers that would have to be able to withstand repeat thermal cycling and large temperature excursions. The light reflected back from the FP cavity is re-collected by the lens and routed to a miniature spectrum analyzer via an optical circulator. A superluminescent diode with a centre wavelength of about  $1560\text{nm}$  was used as a light source. A schematic of the sensor is shown in Fig.1.

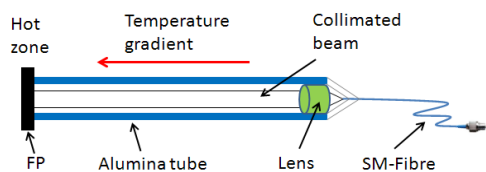


Fig.1: Schematic of temperature sensor



Fig.2: a) Mounted sensor prototype b) Embedded TC and heating coils

In the prototype builds we used alumina tubes of about  $20\text{cm}$  length and  $4\text{mm}$  diameter together with  $\sim 100\mu\text{m}$  thick sapphire plates. Fig.2a shows the front end of the sensor when mounted through the side wall of the furnace.

Temperature measurement is facilitated by monitoring the Optical Path Difference (OPD) of the FP cavity, the temperature dependence of which is given by

$$\Delta(OPD) = 2d \left( \frac{dn}{dT} + \alpha n \right) \Delta T, \quad (1)$$

where  $dn/dT$  is the thermo-optic coefficient of sapphire and  $\alpha$  is the coefficient of linear thermal expansion (CTE) of sapphire. The OPD is derived from the spectrum using, e.g. simple curve-fitting or a cross-correlation method [7].

### 3. Test set-up and initial observations

The sensor was tested in a high-temperature furnace that is controlled via an internal PID controller using an R-type TC embedded in an alumina tube mounted inside the furnace. In addition, an N-type TC was placed in close vicinity to the sensor intended as a reference sensor. A Labview program was used to automatically control the temperature settings and to record and analyze the optical return spectrum. Fig.2b shows the embedded R-type TC together with the heating coils inside the furnace.

At the beginning we checked the quality of the optical return signal over the intended temperature range from room temperature (RT) up to 1300°C. Fig.3 shows the measured spectra at the two extreme temperature ends, demonstrating that an excellent fringe contrast can be maintained throughout.

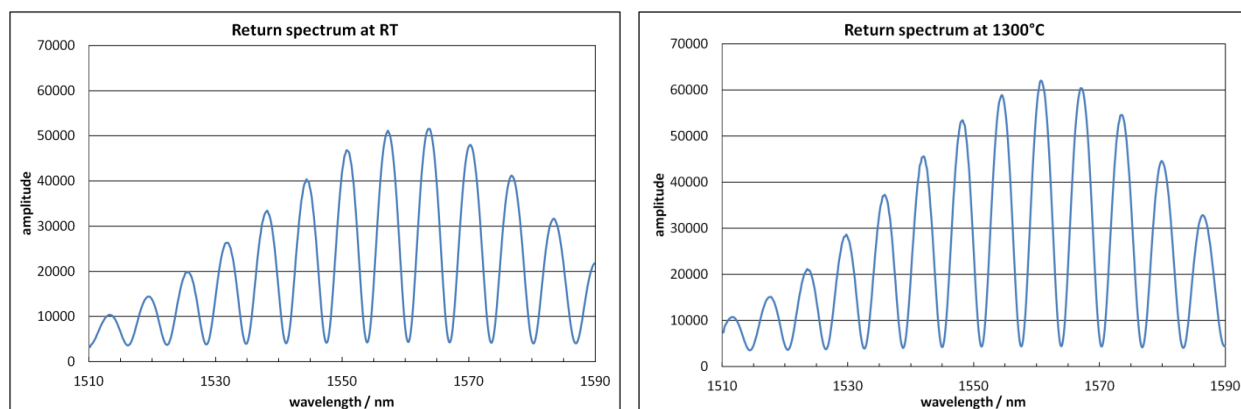


Fig.3: a) Recorded return spectrum at RT

b) Recorded return spectrum at 1300°C

### 4. Test results

**4.1 Temperature calibration:** Between RT and 700°C it was difficult to maintain a stable furnace temperature as the PID circuit is optimized for temperatures above 700°C. Therefore, accurate temperature calibration was restricted to temperatures between 700°C and 1300°C. The temperature was increased in steps of 100°C with a 5hr dwell time at each temperature. As the N-type TC showed increasing noise at higher temperatures (thought to be due to ground loop issues) the embedded R-type furnace TC has been used as a reference for the measurements reported below. Average values of both the furnace temperature and the OPD measurements were taken at each temperature step to create the calibration curve.

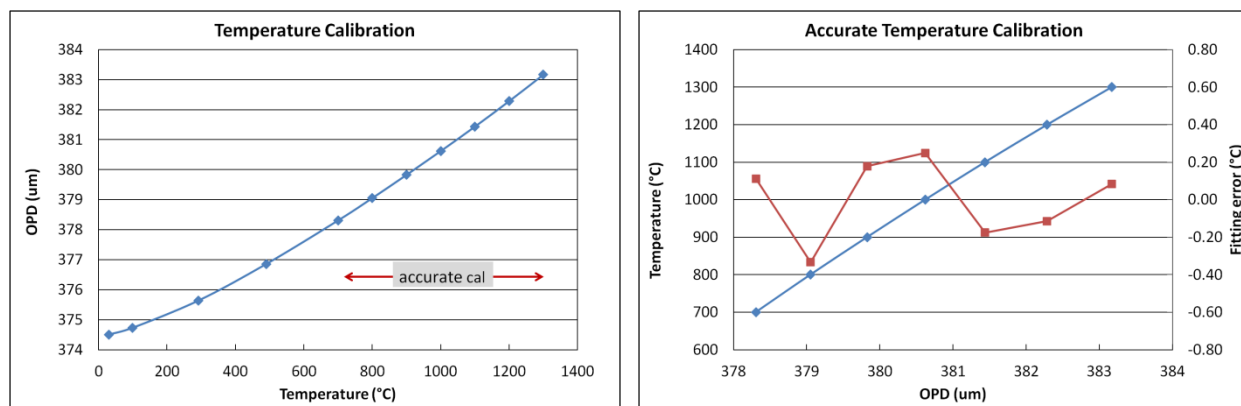


Fig.4: a) Calibration over entire temperature range

b) Accurate calibration between 700°C and 1300°C

Fig.4a is a plot of the calibration curve over the entire temperature range, showing a significant increase in responsivity from RT to 1300°C. This non-linear behavior can be attributed to the fact that both the CTE and thermo-optic coefficient of sapphire are not constant but vary with temperature. A simple quadratic fit between 700°C and 1300°C yields a fitting error of  $< \pm 0.3^\circ\text{C}$  as shown in Fig.4b.

4.2 *Temperature cycling*: Temperature cycling was carried out in the range between 700°C and 1300°C and two full cycles have been completed. Fig.5 shows that the accuracy error is contained between  $\pm 1.5^\circ\text{C}$ .

4.3 *Long-term stability testing at 1100°C*: The furnace was kept at a constant temperature of 1100°C and outputs from both optical sensor and reference TC were recorded once per hour over a period of 42 days. From Fig.6 it is evident that the sensor maintained excellent stability to within  $< \pm 1^\circ\text{C}$  for the whole duration of the test.

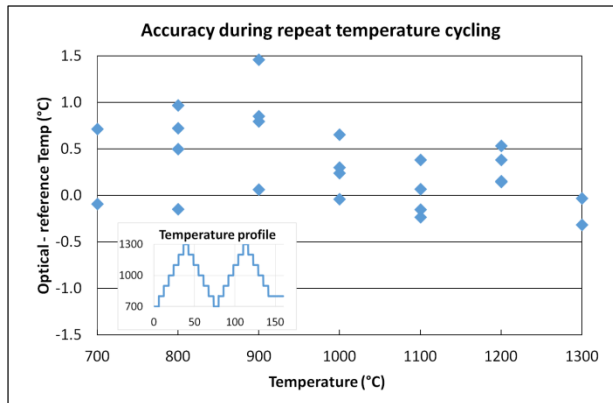


Fig.5: Measurement error during temperature cycling

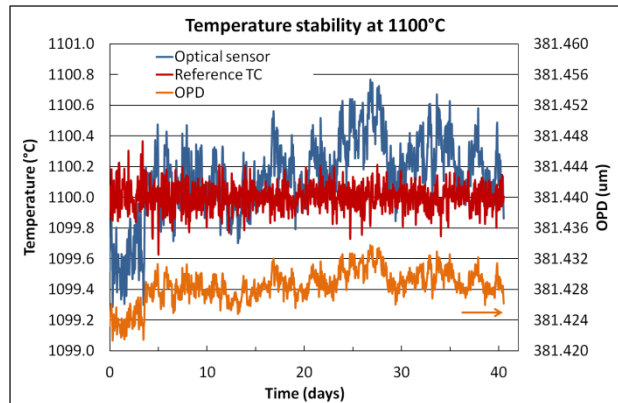


Fig.6: Long-term stability test at 1100°C

4.4 *Long-term stability testing at 1300°C*: After the successful stability test at 1100°C we decided to repeat a similar test at 1300°C. From Fig.7 one can see that the optical sensor experienced an initial downward drift of about

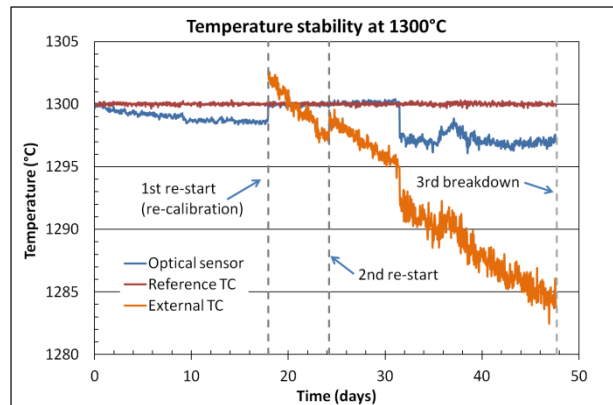


Fig. 7: Long-term stability test at 1300°C

Furnace Break down	Period between failures	Problem
1	18 days	Overprotection TC extension leads
2	6 days	Reference TC
3	24 days	Ref TC circuit problem

Table1: List of furnace TC failure modes

-1.5°C, but stabilized after about 9 days. After 18 days of testing the furnace broke down due to corrosion of the overprotection TC extension leads. As a result of the furnace being repaired the optical sensor had to be repositioned and a re-calibration was carried out. In addition, the ground-loop problem of the external N-type TC was reduced and readings were now included in the records. Noticeable, the TC exhibited a significant drift at 1300°C right from the start of the recordings after it had been exposed to 1100°C for 6 weeks during the first drift test. A further 6 days into the test the furnace reference TC broke down, but this could be replaced and the furnace restarted without changing the optical sensor location. After a further 8 days into the test a sudden drop in temperature of about 3°C was observed in both the optical sensor and the external reference TC, the step being clearly visible in the TC despite it drifting. The fact that two independently operating sensors did record the same temperature jump simultaneously is leading us to believe that this drop may be real despite the fact that the embedded reference TC did not register it. After this the optical sensor remained stable to within  $\pm 1.5^\circ\text{C}$  for the remaining 16 days of the test, which was terminated due to a developing furnace reference TC circuit problem. Despite the difficulties in

carrying out an accurate long-term test at 1300° we are encouraged that the optical sensor stabilized after some initial drift and remained stable to within 3°C over the entire test period of 48 days.

**4.5 Resolution test at 1300C:** For this test the sensor was re-positioned in the furnace and an R-type external TC was used as a reference. The reference TC was placed in direct contact with the sensor alumina tube in close proximity to the sapphire plate as shown in Fig.8. In order to estimate the minimum detectable temperature change at high temperatures the sensor was brought up to a steady state temperature of ~1300°C, followed by a step change of 0.5°C applied to the furnace temperature.

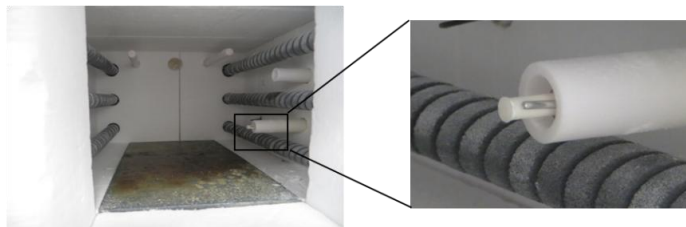


Fig.8: Mounting of optical sensor and external R-type TC

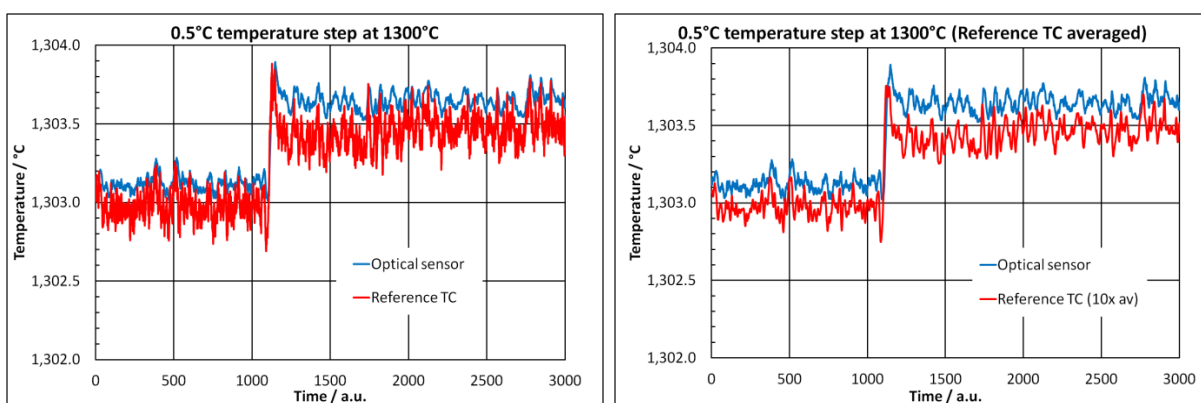


Fig.9: Response to 0.5°C step change a) raw data

b) Reference TC 10x averaged

Fig.9a shows measurements taken at 1.25Hz update rate and reveals that the 0.5°C step is clearly discernible in the time domain. Interestingly, the optical sensor is less noisy than the TC. Applying a running average over 10 points to the TC data reduces the TC noise and reveals a good correlation between the optical and TC measurements (Fig.9b). In fact, there is almost a one to one correlation, indicating that the recorded temperature fluctuations are predominantly real temperature variations rather than caused by system noise.

## 5. Summary

A high-temperature prototype fibre optical temperature sensor based on a sapphire Fabry-Perot transducer element has been demonstrated up to 1300°C. The sensor showed excellent stability  $< \pm 1^\circ\text{C}$  at 1100°C over 42 days and was stable to within 3°C at 1300°C over 48 days. A resolution of  $< 0.5^\circ\text{C}$  was demonstrated at 1300°C without any averaging. The prototype could form the basis for a number of industrial applications.

## 6. Acknowledgements

The authors would like to acknowledge support via the EU funded ASHLEY project for the initial part of the work.

## 7. References

- [1] M. Scervini, "Drift of nickel based mims thermocouples at temperatures above 1000°C: the effect of thermocouple diameter", XXI IMEKO World Congress "Measurement in Research and Industry" August 30 - September 4, (2015), Prague, Czech Republic.
- [2] D. Polyzos et al, "Optical Fibre Fabry-Pérot Sensor Stability at High Temperatures," Proc SPIE **10323**, 103231S (2017).
- [3] A.H. Rose, "Devitrification in Annealed Optical Fiber," JLWT **15**, 808 (1997).
- [4] T. Habisreuther et al, "Sapphire fiber Bragg gratings for high temperature and dynamic temperature diagnostics," Applied Thermal Engineering **91**, 860 (2015).
- [5] Elsmann et al, "Inscription of first-order sapphire Bragg gratings using 400nm femtosecond laser radiation," Optics Express **21**, 4591 (2013).
- [6] D.A. Jackson, "High temperature sensors exploiting low coherence signal recovery," Proc. SPIE **7004**, 70040T, (2008).
- [7] J. Zhenguo, Y. Qingxu, "White light optical fiber EFPI sensor based on cross-correlation signal processing method," Proc. 6th Int. Symp. Test and Measurement, Dalian, China, 1-4 June 2005, **4**, 3509 (2005).